PNNL-38233
M3LW-25OR0404033

Light Water Reactor Sustainability Program

Evaluation of Damage in Medium Voltage Cable Using Machine Learning

September 2025

U.S. Department of Energy
Office of Nuclear Energy

PNNL-38233
M3LW-25OR0404033

Evaluation of Damage in Medium Voltage Cable Using Machine Learning

S.W. Glass, J.R. Tedeschi, M. Elen, M. Taufique, L.S. Fifield
Pacific Northwest National Laboratory

J.A. Farber, A. Kaforey
Idaho National Laboratory

September 2025

Prepared for the
U.S. Department of Energy
Office of Nuclear Energy

Page intentionally left blank

SUMMARY

Developments in cable test instrumentation coupled with artificial intelligence and machine learning (ML) to aid in interpretation of cable test signals supports the feasibility for automated analysis of reflectometry tests for low voltage power cables. This work seeks to leverage prior ML work and success for low voltage cables to evaluate potential application to medium voltage (2 kV to 10 kV) installations. The Accelerated and Real-Time Environmental Nodal Assessment (ARENA) Cable Motor Test Bed at Pacific Northwest National Laboratory (PNNL) was used to test a medium voltage cable with several types of damage including thermal aging and low resistance conductor-to-shield faults. The cable was tested using an inductive clamshell coupler to protect the test instruments from the energized cable voltages that would damage the instruments if coupled directly to the energized conductor. Both unsupervised and supervised ML methods were applied. Observations and conclusions include:

- Model extension to assess reflectometry signals from cables of different lengths based on several normalization strategies proved problematic. Visually, the alignment of cables using dynamic time warping (DTW) was successful. However, damage prediction accuracy fell below 50% when using the unsupervised method and ranged from 22 to 61% using the supervised method. We suspect that the actual noise from damaged portions of the cables was aligned with the random noise that can be seen in all cables, making damaged cables difficult to distinguish from undamaged cables. This is particularly important for supervised learning approaches where good cable and damaged cable training data are likely to be from different cable lengths. This is less important for unsupervised approaches that will normally look for changes to that baseline from baseline data obtained when first connecting to the cable of interest.
- The unsupervised model achieved a maximum weighted accuracy of 93.8% using the vector network Analyzer (VNA) Frequency Domain Reflectometry (FDR) Direct Connect data at 100 MHz with real preprocessing. The analysis indicated that Direct Connect and Iso-Coupled Unenergized methods produced significantly higher accuracy compared to other connection methods. Furthermore, higher frequencies correlated with better performance, especially when using the Direct Connect and Iso-Coupled Unenergized methods. Among preprocessing methods, real and imaginary preprocessing performed best, while the complex magnitude preprocessing method performed the worst.
- Overall, this study demonstrates that the unsupervised ML methods previously developed for low voltage cables extend effectively to medium voltage cables, showcasing the robustness of the framework and approaches. These findings can serve as a guideline for commercial applications, aiding in the development of technologies that enable efficient and effective cable condition monitoring and condition-based qualification of cables, ultimately enhancing the reliability and safety of nuclear power plant operations.

ACKNOWLEDGEMENTS

This work was sponsored by the Department of Energy, Office of Nuclear Energy, for the Light Water Reactor Sustainability (LWRS) Program Materials Research Pathway. The authors extend their appreciation to Pathway Lead Dr. Xiang (Frank) Chen for LWRS programmatic support. This work was performed at the Pacific Northwest National Laboratory (PNNL) and at the Idaho National Laboratory (INL). PNNL is operated by Battelle for the U.S. Department of Energy under contract DE-AC05-76RL01830. INL is operated by Battelle Energy Alliance, LLC, for the U.S. Department of Energy under Contract DE-AC07-05ID14517. This report is submitted as the deliverable for milestone M3LW-25OR0404033.

Page intentionally left blank

CONTENTS

FIGURES

Page intentionally left blank

ACRONYMS

AC	alternating current
ARENA	Accelerated and Real-time Environmental Nodal Assessment
AWG	arbitrary waveform generator
BPSK	binary phase shift keying
BW	bandwidth
C&I	control and instrumentation
CEA	Commissariat à l'Energie Atomique et aux Energies Alternatives
CNN	convolutional neural network
CWF	composite waveform
dB	decibel
DC	direct current
DOE	U.S. Department of Energy
dt	Decision Tree Classifier (ML algorithm)
DTW	dynamic time warping
EAB	elongation-at-break
EPR	ethylene-propylene rubber
ETC	Extra Trees Classifier (ML algorithm)
Fc	carrier frequency
FDR	frequency domain reflectometry
FFT	fast Fourier transform
LWRS	Light Water Reactor Sustainability
MCTDR	multi-carrier time domain reflectometry
ML	machine learning
MLP	Multi-Layer Perceptron Classifier (ML algorithm)
NDE	non-destructive evaluation
NPP	nuclear power plant
NRC	Nuclear Regulatory Commission
OMTDR	orthogonal multi-tone time domain reflectometry
PN code	pseudo-random noise code
PNNL	Pacific Northwest National Laboratory
PV	photovoltaic
RF	radio frequency
SMOTE	Synthetic Minority Over-sampling TEchnique
SSTDR	spread spectrum time domain reflectometry
SVM	Support Vector Machine linear kernel (ML algorithm)
TDR	time domain reflectometry
VAE	variational autoencoder
VNA	vector network analyzer

Page intentionally left blank

1. INTRODUCTION

In accordance with guidelines and standards specified in the U.S. Nuclear Regulatory Commission (NRC) Guide 1.131 (NRC 1977) and IEEE 383 (IEEE 2015), nuclear power plant (NPP) safety-critical cables are initially qualified for 40 years. However, most NPPs in the United States have applied for or have been granted life extensions beyond their initial 40-year license. For extension of cable qualified life to 60 years in reactor license renewal and to 80 years in subsequent license renewal, where possible, licensees have utilized re-analysis of the original qualification data and conservatism present in the original methodology to extend cable qualified life to 60 and to 80 years, respectively. When the original time-based qualification period (e.g., 40 years) comes to an end, and conservatisms and margins of the time-based qualification have been consumed so that the qualification period can no longer be extended through re-analysis, the continued qualified status of the cable must be pursued using a different method. This is the case whether the time at which re-analysis is no longer viable falls within the first period of license renewal (40 to 60 years), the second period of license renewal (60 to 80 years), or later. As outlined in the latest NRC-endorsed standard for qualification, IEEE 383-2015, (IEEE 2015), options for an operator at the end of the qualified life of a cable in addition to re-analysis and use of conservatism include type-testing of service-aged cables, re-qualification of cables to the extended period of operation, replacement of the cable that has come to the end of its qualified life with a new cable , and pursuit of condition-based qualification Interest in the last option is growing as plants age. The paradigm shift to use of tested condition rather than time as the basis for confidence in the ability of a cable to perform its safety-related function (IAEA 2017) is attractive do the cost and complexity of replacing installed cables at the end of their qualified life and because experience has shown that cables can continue to function safely well beyond their initial qualification.

In current cable aging management, testing is normally performed during plant outages when the cables can be taken out of service. Reflectometry techniques, including time domain reflectometry (TDR), frequency domain reflectometry (FDR), and spread spectrum time domain reflectometry (SSTDR), are among the tools currently available to assess cable condition offline (Glass et al. 2015). Such offline tests typically require cables to be de-terminated at one or both ends, or at least to have insulation peeled back near a cable end to allow contact with the conductor. Removing a component or system from service for testing, exposing the conductor, performing the test, then reconnecting the cable is also costly and exposes the system to potential workmanship and operator errors during testing. The high frequency/low voltage nature of reflectometry tests, however, also offers the promise of potentially performing the task while the cable is online and energized under certain conditions. Pacific Northwest National Laboratory (PNNL) has demonstrated that an inductive coupler can be applied to low voltage and to medium voltage cables at voltages of 10 kV or greater, DC or 60 Hz, safely allowing the high frequency reflectometry test instruments to interrogate the cables without being damaged (Glass et al. 2024a; Glass et al. 2025).

Although reflectometry techniques are shown to be able to detect a wide range of cable damage, the signals are also known to be complex, noisy, and challenging to visually interpret. Machine learning (ML) methods have been successfully applied to mitigate this concern by distinguishing good or undamaged cable reflectometry signals from damaged or anomalous reflectometry signals.

The Commissariat à l'Energie Atomique et aux Energies Alternatives (CEA) has been engaged in research on reflectometry and ML applications for cable diagnostics (Slimani et al. 2024). Their work includes the development of non-intrusive reflectometry methods, such as multi-carrier time domain reflectometry (MCTDR) and orthogonal multi-tone time domain reflectometry (OMTDR), which are designed to operate without interfering with the native signals of the system being tested. In the 2024 study, CEA researchers proposed an ML approach for classifying faults in cables using compressed sensing time domain reflectometry. The study demonstrated the effectiveness of supervised ML models in identifying fault types and their locations with high precision. Additionally, unsupervised clustering

techniques were employed to preprocess reflectometry data, significantly boosting the accuracy of fault detection. The CEA research highlights the potential of ML to enhance the diagnostic capabilities of reflectometry systems.

Dr. Joel Harley of the University of Florida has contributed to the application of ML in reflectometry-based diagnostics. His work focuses on using supervised and unsupervised dictionary learning techniques to analyze SSTDR data. In a 2020 study (Edun et al. 2021), Harley and his team applied these methods to fault detection in photovoltaic (PV) systems, demonstrating their effectiveness in identifying cable anomalies. The researchers also explored the use of SSTDR for measuring capacitance and complex impedance, employing steepest descent inversion techniques to enhance the accuracy of their measurements. By integrating ML algorithms, they were able to automate the interpretation of reflectometry data, reducing the need for manual analysis and improving diagnostic efficiency. This work provides a strong foundation for extending ML-aided SSTDR techniques to medium voltage cables (Kingston et al. 2021).

Two additional studies (Edun et al. 2021; Edun et al. 2022) used SSTDR to detect, isolate, and characterize anomalous data (or faults) in a PV array. The test setup was a five-panel array with a 59.13 m leader cable. The goal was to learn the distribution of non-faulty input signals, inspect the reconstruction error of test signals, flag anomalies, and then locate or characterize the anomalous data using a predicted baseline rather than a fixed baseline that might be too rigid. The first study used traditional unsupervised learning methods and the second used a Variational Autoencoder (VAE), which handled imbalanced data better than other methods used for classification of PV faults because of its unsupervised nature. For detecting cell disconnects within the PV array, an overall accuracy of 96% was found for detecting true negatives (non-faulty data). The true positive rate for detecting anomalies was 0.99% and the area under the Receiver Operating Characteristic curve was 0.99. The fault location error was within 0.40% for the five-panel test setup. This work showed that the VAE machine learning approach readily detected and located faults of interest in a simple test setup.

Lee and Chang (Lee and Chang 2020) examined the integrity and functionality of control and instrumentation (C&I) cable systems using an ML approach. Neural networks and a hierarchy clustering algorithm were used for fault detection and identification of the faulty line. The proposed clustering algorithm was verified via experiments with four possible fault scenarios using automotive wires and control and instrumentation cables for NPPs. The algorithms were found to accurately detect and estimate fault locations.

Other studies have validated the practical use of ML-aided reflectometry systems for cable diagnostics. A 2021 study by Lim et al. (Lim, Kwon, and Shin 2021) demonstrated the effectiveness of time-frequency domain reflectometry combined with ML algorithms for fault detection and localization in shielded cables. The researchers employed optimal detection techniques to enhance the resolution and accuracy of their measurements.

A study by Robles et al. (Robles, Shafiq, and Martinez-Tarifa 2019) focused on multiple partial discharge source localization in power cables using power spectral separation and TDR. By integrating ML models, the researchers were able to distinguish between different discharge sources, providing valuable insights into cable health. These findings underscore the potential of ML-enhanced reflectometry for addressing complex diagnostic challenges in medium voltage systems.

The U.S. Department of Energy (DOE) Light Water Reactor Sustainability (LWRS) program has made significant contributions to the field of cable non-destructive evaluation (NDE) particularly focusing on reflectometry methods. Initial work focused on low voltage (600 V) cables for offline detection and location of cable faults and anomalies (Glass et al. 2017; Glass et al. 2021; Glass et al 2022). Commercial SSTDR instruments and methods for online testing of aircraft and rail cables have been available for more than a decade but these instruments have been limited to 1000 V (Furse 2006; Furse and Woodward 2003). The potential for online cable tests of power cables including medium

voltage (to 10 kV and higher) was explored by the LWRS program team with development of an inductive clamshell coupler for cable reflectometry tests (Glass et al. 2024a; Glass et al. 2025).

The possibility of performing cable diagnostic tests on energized lines as a component of the cable aging management program of a power plant highlighted the need for an effective automated way to evaluate the test signals. Reflectometry data is notoriously complex and generally cannot be evaluated by simple threshold alarms. The LWRS program explored both supervised and unsupervised machine learning methods to examine unshielded and shielded power cable for low-resistance phase-phase and conductor shield faults (Glass et al. 2024b; Glass et al. 2024c). Conclusions from this work were that both supervised and unsupervised machine learning methods applied were effective at identifying and distinguishing between good cable and damaged or anomalous cable in reflectometry tests. The work was extended to address continually varying reflectometry test signals associated with thermal aging. A portion of a representative shielded 600 V-rated power cable was aged at 140°C for 70 days and reflectometry data was captured during the aging period. Witness samples were also extracted for elongation-at-break (EAB) destructive tests to correlate with the reflectometry tests. The unsupervised learning analysis results indicated a strong correlation between the anomaly score and EAB. The Spearman correlation analysis to assess the correlation between unsupervised damage predictions and EAB showed a score of -0.84. As an example of the unsupervised ML analysis, the FDR examination using the inductive clamshell isolation coupler on an energized cable and restricting the data to just the real part (as opposed to considering both real and imaginary FDR components) and averaging the 200 and 400 MHz results, a weighted accuracy of 89.6% was achieved. The supervised learning weighted accuracy for the same data was 0.94%. This suggests that ML can be used to distinguish damaged cables from undamaged cables at the standard threshold of 50% EAB. It was noted that unsupervised approaches seemed more practical for field implementation as they did not require substantial human intervention to pre-classify training data. Tests were performed on both unenergized and energized cables and the energized tests resulted in only slight reductions in the weighted accuracy predictions.

This LWRS program study is an extension of prior work to apply the low-voltage cable test developed machine learning to a medium voltage cable.

2. TEST SETUP AND DATA ACQUISITION

Generally, the Accelerated and Real-time Nodal Assessment (ARENA) Cable Motor Test Bed (www.pnnl.gov/arena) was used to acquire data on a medium voltage cable using both FDR and SSTDR techniques. The test bed, an overview of the reflectometry methods, and a more detailed explanation of the inductive clamshell coupler that is essential to allow data acquisition on energized cable are provided below.

2.1 ARENA Cable Motor Test Bed

To evaluate the degradation of electrical cables and particularly the interaction of electrical cable test technologies with various damage mechanisms PNNL developed the ARENA test bed (Glass, Fifield, and Prowant 2021) shown in Figure 1. The vision behind the creation of this capability is to establish a modular test facility that allows for the implementation of a broad range of test methods to detect faults and anomalies in a variety of cables and systems in a controlled environment. ARENA includes:

- A motor controller for 3-phase 480 VAC motor control
- A ½ horsepower 3-phase 480 VAC motor
- Remote start and barriers to protect operators from arc-flash exposure should a cable fail
- Circuit breaker protection to guard and isolate the building power from test system failure

- A thermal aging oven that allows up to 10 m of cable to be spooled and thermally aged
- A water bath that allows cables to be submerged
- Cable trays like those found in NPPs to allow cables to be spread and protected from operators standing on the cables or moving them during testing
- A Tan Delta test instrument by HV Diagnostics used to energize the medium voltage cable (not connected to the motor so there was essentially no current flowing)
- A PNNL developed 2 kV transformer setup.

The system can be operated with either shielded or unshielded cable.

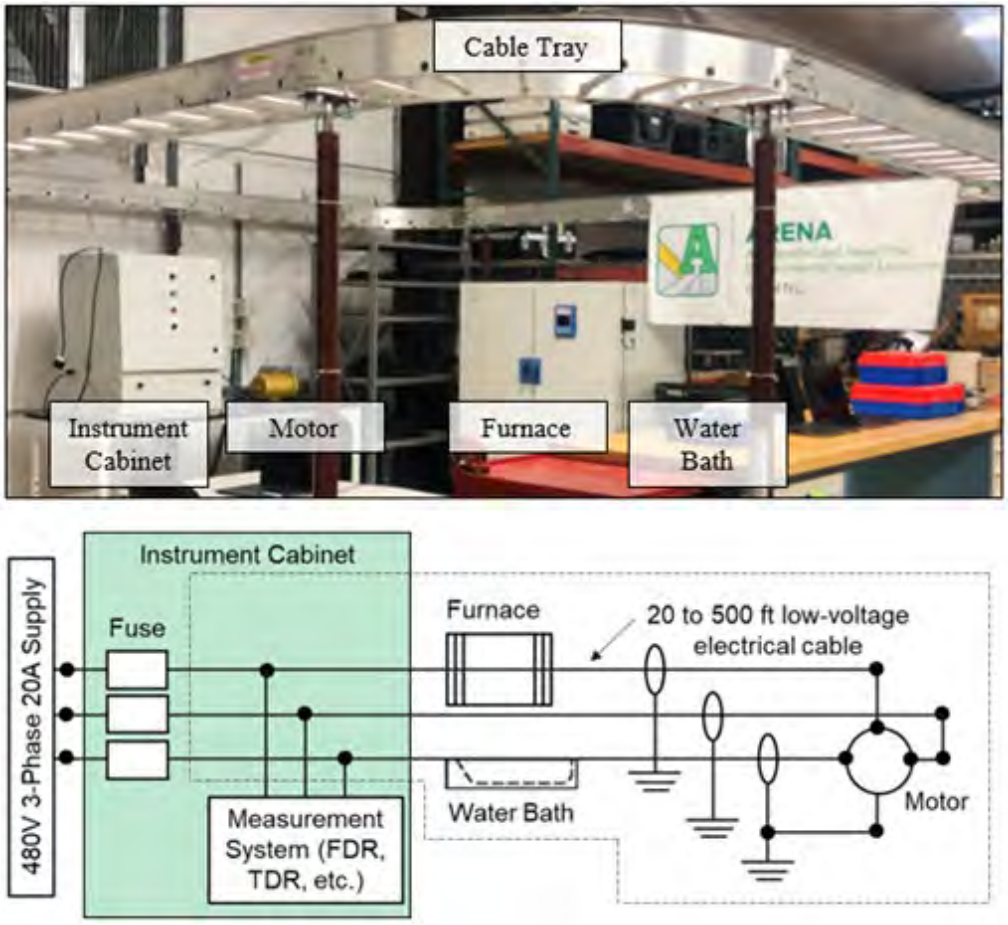

Figure 1. The ARENA Test Bed (top) digital image and (bottom) schematic (Glass et al. 2023).

2.2 Frequency Domain and Spread Spectrum Time Domain Reflectometry

In this study, FDR and SSTDR tests were considered. With both FDR and SSTDR, the reflectometer test instrument is connected to the cable end and a voltage wave is applied to travel along the cable. The FDR instrument is a vector network analyzer (VNA) and the SSTDR instrument set uses an arbitrary waveform generator and a digitizing oscilloscope to transfer data to a computer running Python script. If an impedance change is encountered by the signal moving along the cable, part of the energy is reflected to the test instrument. The indication location is related to the distance along the cable by the wave velocity of propagation. Reflectometry methods utilize high frequencies and so are candidates for high

frequency isolation from DC or low frequency (50/60 Hz) line voltages. This makes them candidates for use with online energized cable tests. Reflectometry tests were conducted on the configuration as shown in Figure 2.

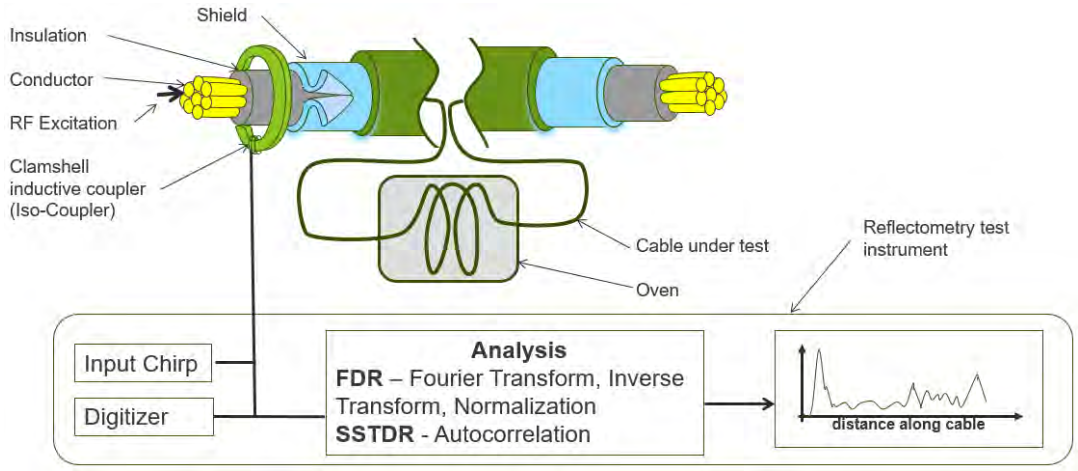

Figure 2. Reflectometry cable test configuration.

2.3 Inductive Clamshell Isolation Coupler

A recent PNNL development is an inductive clamshell isolation coupler (also referred to as the Iso-Coupler) that allows FDR and SSTDR measurements to be made on energized cable (Glass et al. 2024a; Glass et al. 2024b). This coupler was not available during the previous ML project and so we were only able to consider testing unenergized cables at that time. For the current project, however, tests using the coupler were among the mix of test conditions to try to establish if the coupler impeded our ability to do reflectometry tests and if testing energized cable vs. unenergized cable affected the results.

The laboratory instrument SSTDR, VNA FDR, and most radio-frequency (RF) instruments are limited to 10–30 V at 60 Hz. Without a protection/isolation circuit, high-voltage direct current (DC) or 60 Hz alternating current (AC) voltage (typically from 120 V to 15 kV) will damage costly RF test equipment. An ideal way to perform these measurements is with a high-pass filter that can suppress DC and 60 Hz low-frequency power voltages and allow higher RFs to pass through. This, however, is not practical to support both high-voltage suppression and passing of high RFs (>100 MHz). Therefore, instead of a classical filter, a current probe that supports reciprocal measurements is used. The commercial current probe can both transmit and receive and can be used to inject and sense RF signals on a live voltage line while providing low-frequency isolation to RF test equipment.

RF current probes are designed based on insight from Ampere-Maxwell equations for alternating currents. In the application of a current probe (see Figure 3**)**, an alternating current along the primary conductor, I_P, will induce a magnetic flux, B, within the core of the ferromagnetic material surrounding the primary conductor. A readout conductor wrapped around the ferrite core can then measure a secondary current, I_s, that is proportional to the number of turns wrapped around the ferromagnetic core, N, and to the primary current. Such current coupling probes are used for commercial applications of measuring current on AC lines for single conductors. The design of the core and number of windings influence the characteristic impendence of the coupler and set the current at which the ferrite core itself will saturate, with specific design considerations such as parasitic capacitance between secondary windings for high-frequency current probes. RF current probes are transformers that measure, or produce, a voltage in a 50-ohm load proportional to the current flowing through the inner diameter of the probe based on the characteristic impedance of the probe. This is referred to as the transfer impedance of the probe and can be used to calculate the insertion loss of the probe vs. frequency (Yao, Ma, and Yu 2014),

$$IL = 20 \log_{10}(R) - Z_T, \qquad \text{Eq. 1}$$

where IL = insertion loss (dB), R = impedance of the RF circuit = 50 ohms, and Z_T = transfer impedance (dB ohms). The insertion loss values through RF probes are in the -40 to -80 dB range for 60 Hz signals and typically better than -10 dB in the MHz frequency range. This approach creates a noncontact, frequency selective mechanism where RF signals can interact with live voltage lines.

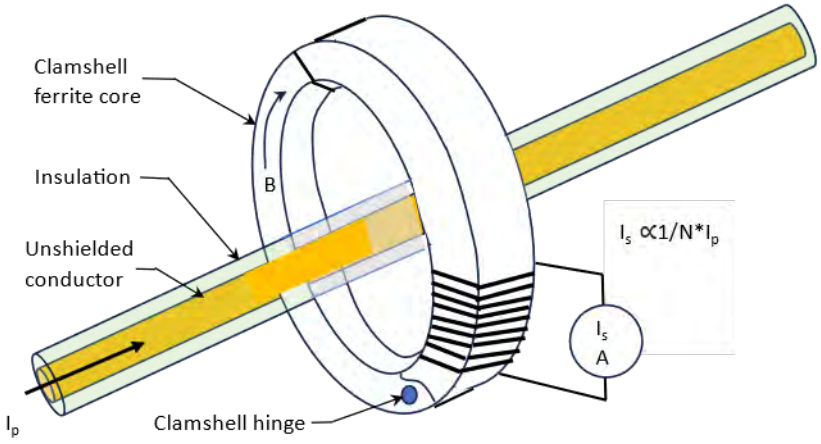

Figure 3. Architecture of a typical current probe.

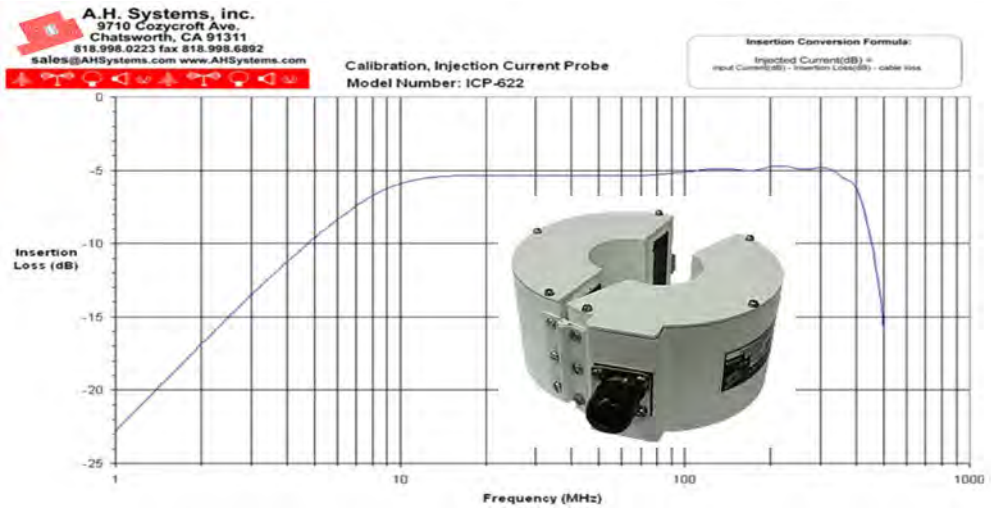

Figure 4. Commercial inductive clamshell coupler (inset) and frequency response.

2.4 Cable and Cable Faults Tested

This study used a 50-ft length of Okonite Okoguard 5 kV Medium Voltage Cable of size 1/0 AWG, with the jacket label printed as "1/C 1/0 CMPCT CU EPRSC OKOS SH 115-024-060 5/8KV FOR CT USE" (Okonite 2019). The outer diameter of the cable was 0.8 in. This cable consists of a copper conductor surrounded by a strand screen, an extruded semiconducting ethylene-propylene rubber (EPR), and an insulation made of Okoguard EPR. Another insulation screen surrounds the strand screen followed by an extruded semiconducting EPR, with shielded copper tape and an Okoseal jacket as the external layer. Various configurations of test equipment were used, and various fault conditions were tested as indicated below. Data using each setup and fault condition were collected from both ends (End A and End

B) of the cable. The excitation source (see Figure 2) used to energize the cable was the Tan Delta equipment from HV Diagnostics that supports variable 0.1 Hz excitation up to 24 kV, and the 2 kV PNNL-built transformer connected to a 60 Hz supply. The control box refers to the setup used to energize the cable, either the HV Diagnostics Tan Delta equipment referred to as “HVD”, or the 2 kV transformer based on the experimental setup. When the cable under test is connected as an energized circuit—either with the HVD instrument or the transformer—the reflectometry signal includes additional peaks from the upstream portion of the circuit that can complicate reflectometry signal interpretation.

Figure 5. Medium voltage cable (The Okonite Company, 115-024-060).

Equipment Used:

- VNA FDR (Copper Mountain 2020)
- PNNL SSTDR (Glass et al. 2023).

Equipment Configuration Used:

- Direct Connect
- Iso-Coupler Un-Energized
- Iso-Coupler Un-Energized with HVD
- Iso-Coupler Energized with HVD
- Iso-Coupler on Outer Jacket - Un-Energized
- Iso-Coupler on Outer Jacket - Un-Energized with HVD
- Iso-Coupler on Outer Jacket - Energized with HVD.

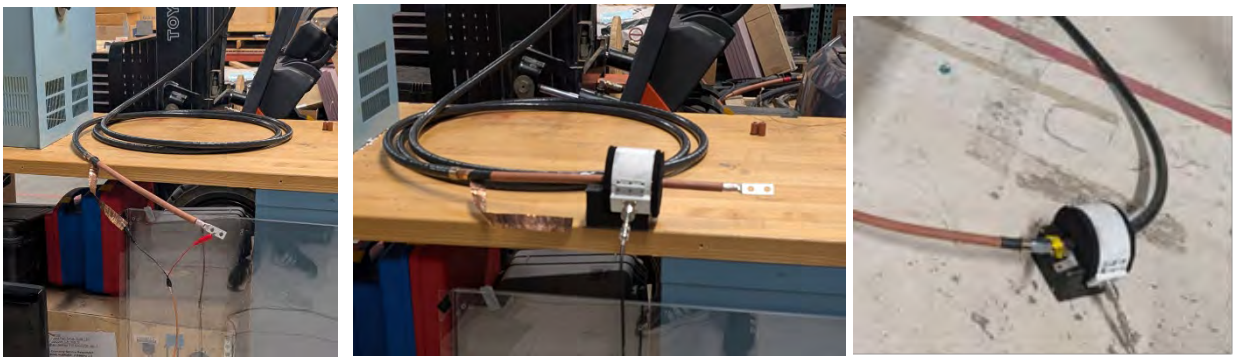

Figure 6. From left to right (a) Direct Connect (b) Iso-Coupler (c) Iso-Coupler on outer jacket.

Fault Conditions:

- Undamaged

- Undamaged with Short at Other End (only for Un-Energized measurements)
- Damaged at 20 ft from End A
- Damaged at 20 ft from End A, with Short at the Other End (only for Un-Energized measurements)
- Ambient Measurement (New Cable)
- Thermal Aging Fault (New Cable).

A different cable sample was used, where a 4 ft segment of the cable was thermally aged up to 45 days in a mechanical convention oven at ARENA as shown in Figure 7. Witness samples were withdrawn every 7 days to monitor the extent of degradation during the aging study. Reflectometry measurements were taken once at ambient conditions on an unaged cable and after 45 days on the aged cable. Indenter modulus measurements were obtained on the intermediate thermally aged insulation specimens, as shown in Figure 8. Further mechanical characterization studies, as well as dielectric spectroscopy studies may be performed using the witness samples in future work.

Figure 7. 4 ft segment of a 50 ft cable, in a thermal aging oven with the witness samples.

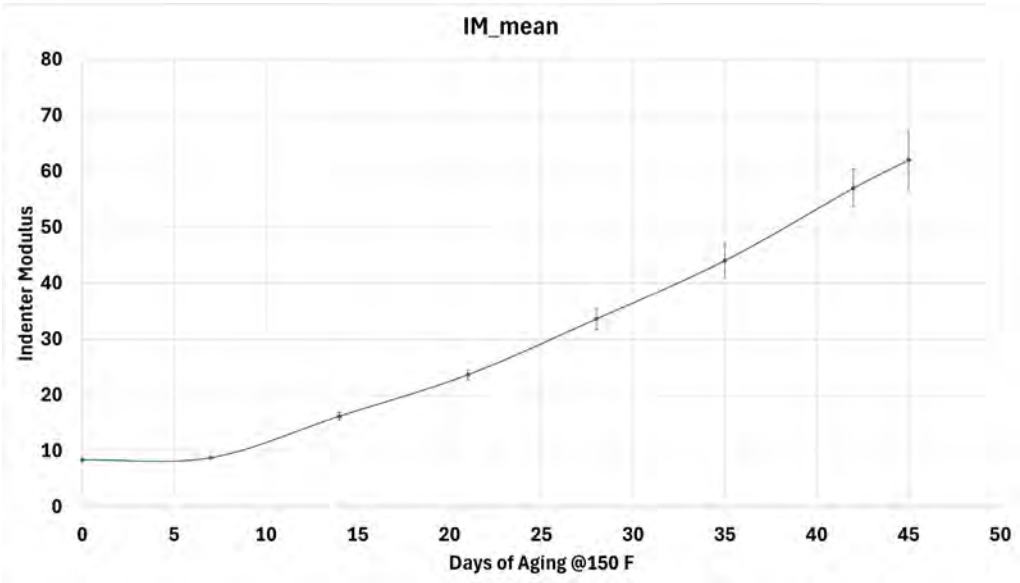

Figure 8. Indenter modulus of thermally aged medium voltage insulation specimens.

It is also important to note that, in our previous work (Glass et al. 2024b), for reflectometry measurements in the low voltage cable, the connections were made between two insulated conductors in a multiconductor cable for the direct connect setup, whereas in this work for the medium voltage cable, the positive is connected to the center conductor and the negative is connected to the outer shield of the medium voltage cable under test. In the case of the Iso-coupler measurements, it is also important to note that, for the low voltage cable, only one of the three conductors was used as the primary cable under test, and for the medium voltage cable, since there is only a single core, the conductor and insulation are tested with the shield stripped back.

3. Visual Image of Reflectometry Data Results

The following figures (Figures 8 - 15) depict the reflectometry responses for the various test cases discussed above. Representative plots are displayed for selected test cases to provide a better understanding of the data collected and how it is processed further. As mentioned above, the cable length is 50 ft with an additional leader cable of 20 ft length. Hence, the first indication of cable under test is observed at ~23 ft, and the end of the cable is observed after ~75 ft in the figures plotted below. The dotted lines in the plots indicate the reflectometry responses for the damaged conditions, where the solid lines represent the responses for the undamaged conditions. Visual differences between the solid and dashed lines are subtle. The hope is that some of the ML signal treatment will be able to distinguish damaged from undamaged test conditions.

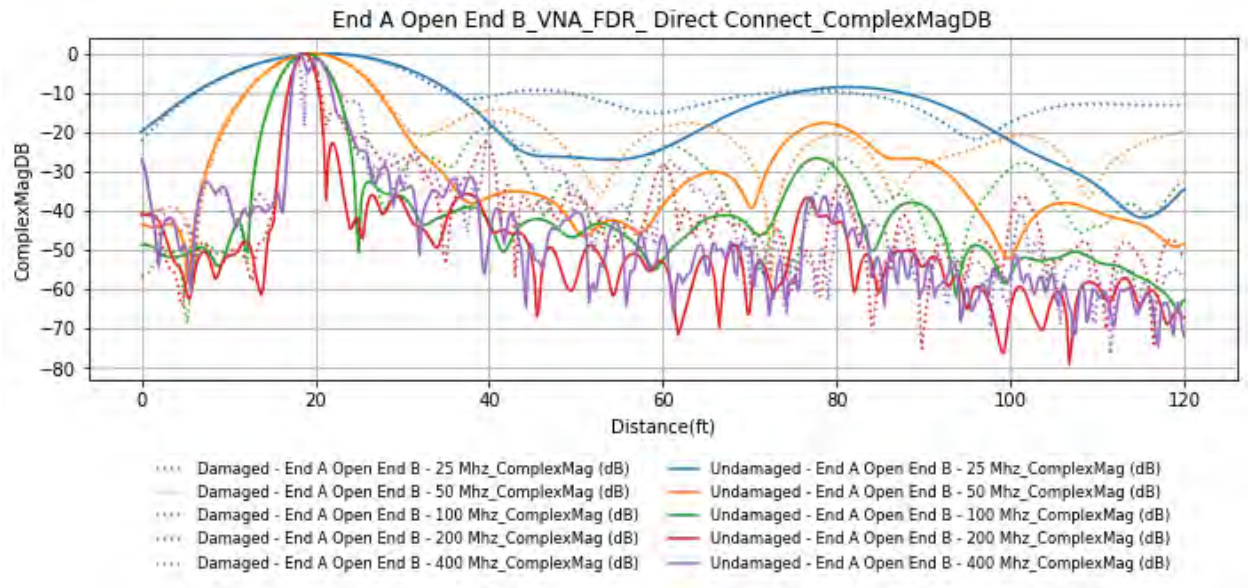

Figure 9. Direct Connect measurements with VNA FDR.

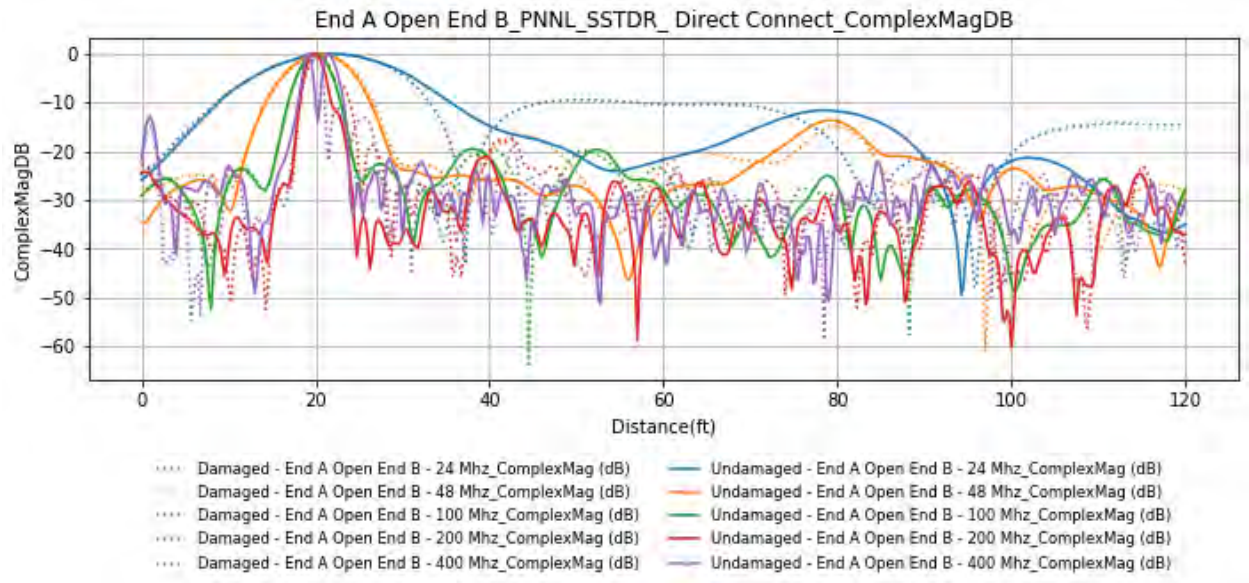

Figure 10. Direct Connect measurements with PNNL SSTDR

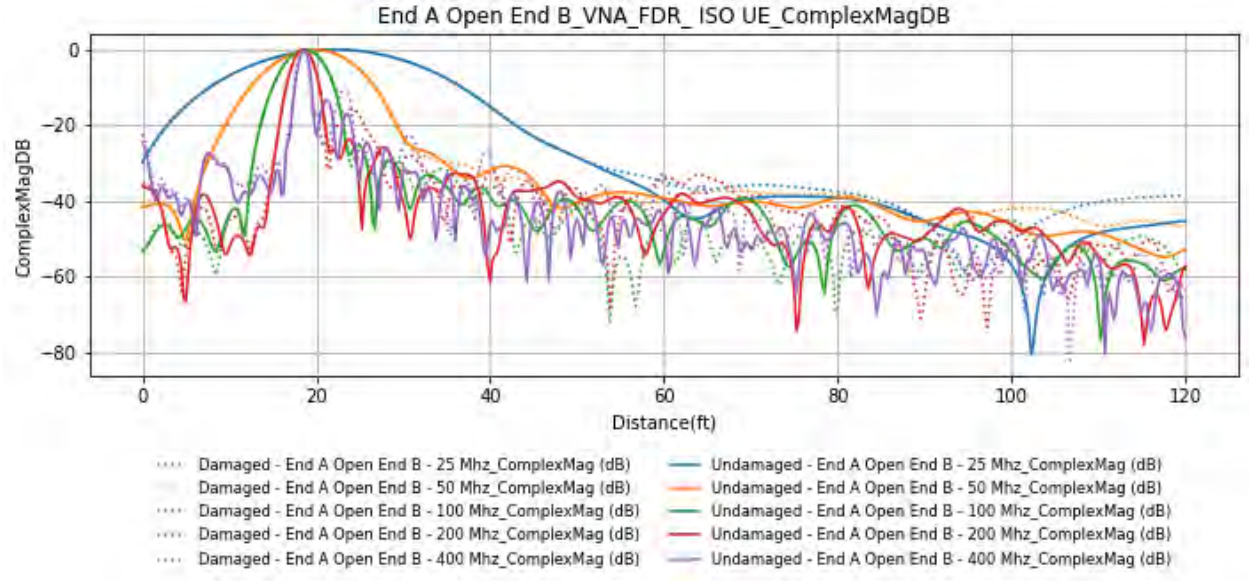

Figure 11. Iso-Coupler un-energized measurements on insulation with VNA FDR.

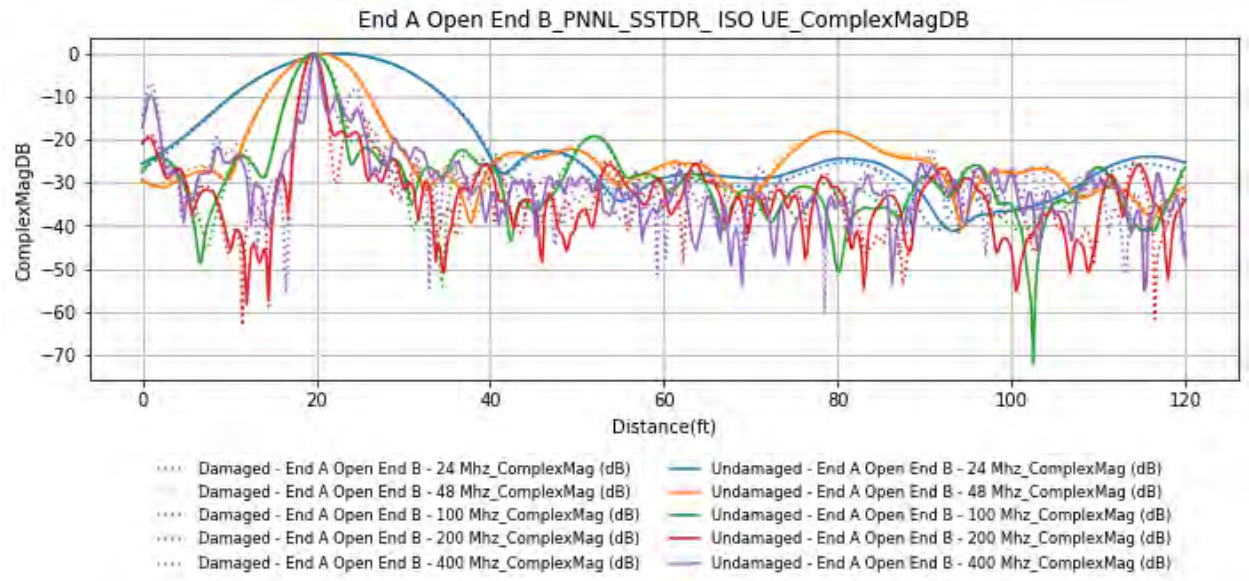

Figure 12. Iso-Coupler un-energized measurements on insulation with PNNL SSTDR.

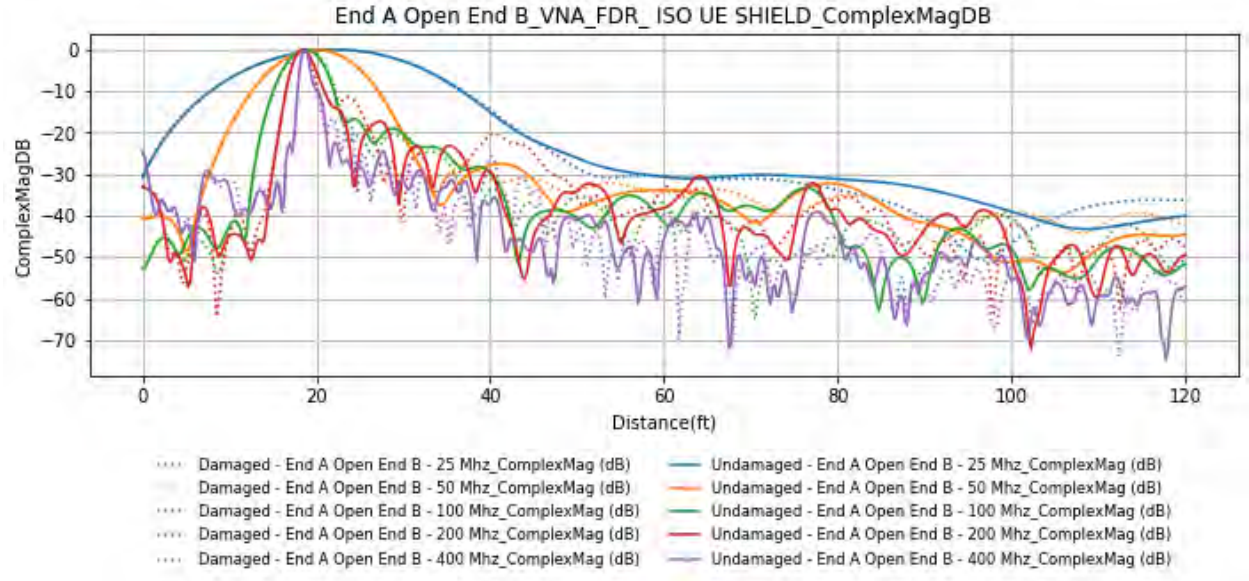

Figure 13. Iso-Coupler un-energized measurements on jacket with VNA FDR.

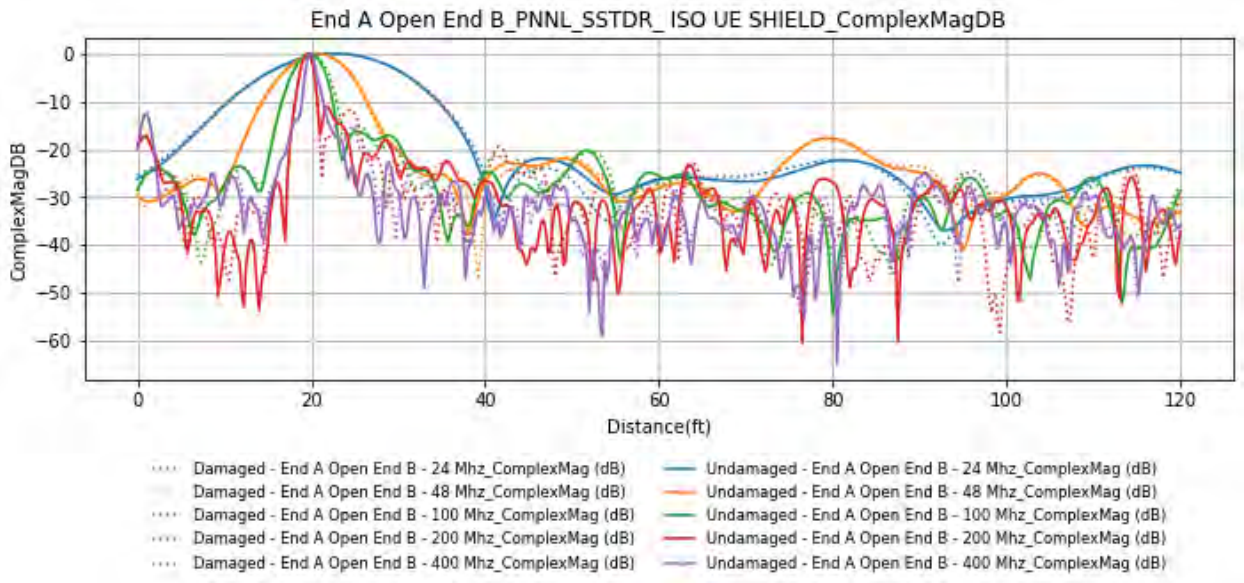

Figure 14. Iso-Coupler un-energized measurements on jacket with PNNL SSTDR.

Figure 15 and Figure 16 depict direct connection reflectometry responses for the unaged vs thermally aged cables.

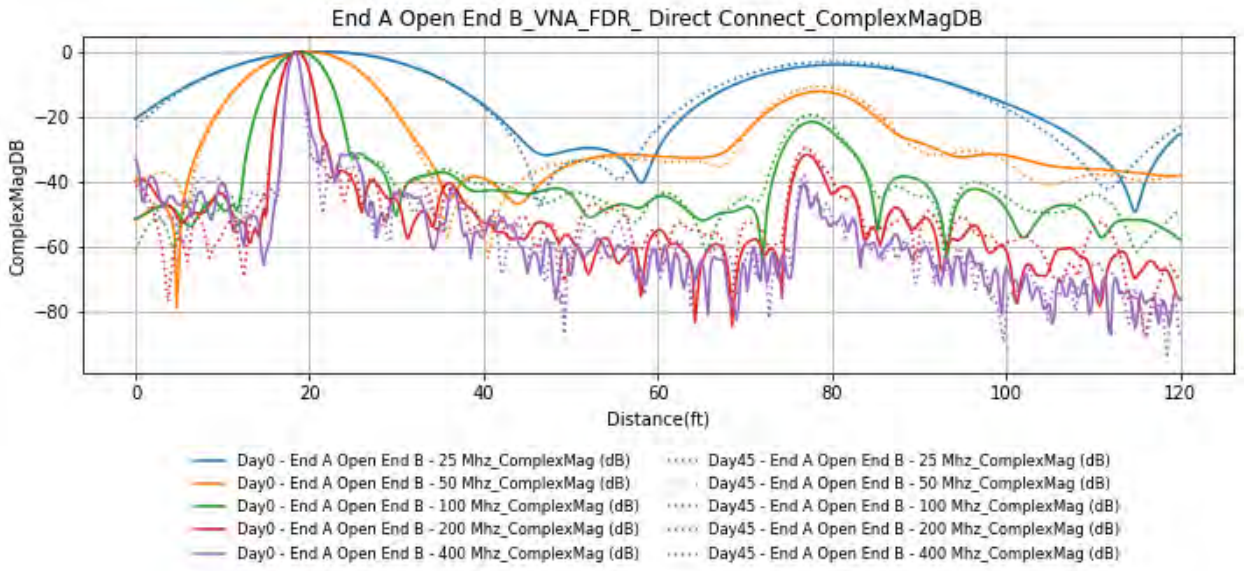

Figure 15. Direct Connect VNA FDR measurement of thermally aged cable.

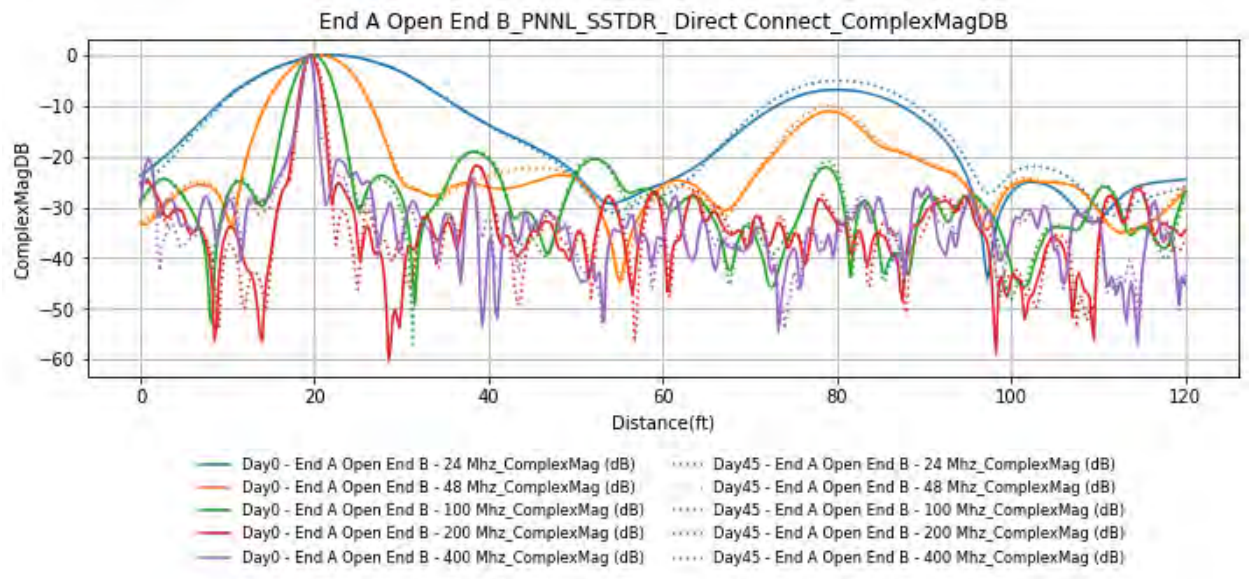

Figure 16. Direct Connect PNNL SSTDR measurement of thermally aged cable.

4. METHODS

This section details the methods employed to process and analyze the collected data, ensuring robust and reliable results. These include preprocessing steps to transform raw waveform data into a suitable format for further analysis, cross validation to improve reliability and generalizability of the models, both unsupervised and supervised methods of classifying the reflectometry signals, and final use of evaluation metrics for comparative purposes.

4.1 Preprocessing

After the initial processing, such as the time-domain and frequency-domain conversion, which happens directly through the batch data collection process established by Python scripts developed at PNNL, the raw data files are obtained in the complex domain, including both real and imaginary components. The data are then transformed in various ways to assess how the transformation process affects classification performance. These processed data then become the input into the ML algorithms described below.

The Normalized Magnitude (A.U.) and Magnitude (dB) are calculated as per the information below:

- Raw data collected – Waveform in the complex domain
  - Waveform = A + iB
- Converted to complex magnitude (dB) and normalized on the highest value.
  - Complex Magnitude (dB) = 20 log (sqrt(A^2+B^2)) – Max (20 log (sqrt(A^2+B^2))
- Converted to magnitude (A.U.) and normalized based on the highest value.
  - Normalized Magnitude (A.U.) = (sqrt(A^2+B^2)) – Max((sqrt(A^2+B^2))

Based on our previous work, it has been observed that the faults are more distinguishable visually in the Normalized Magnitude (A.U.) plots.

Additionally, based on the data-processing procedure established in our previous work (Glass et al. 2024c), the Composite Wave Form (CWF) is calculated as the mix of the lower and higher frequency bandwidths by multiplying them. This process reduces the noise and accentuates the reflections of interest.

4.2 Cross-Validation Strategy

In most ML applications, data are split into training and testing sets to evaluate the model using data that it has not been trained on to avoid artificially high performance not achievable in a production environment. Based on this concept, cross-validation is a technique to reduce the impact that a particular train/test split can have on the resulting accuracy. It works by splitting the data multiple times and combining (e.g., by averaging) the results. A common method of cross-validation is k-fold cross-validation, in which the data are split into k parts. For k iterations, one part is withheld as the test set while the rest of the data is used for training. Then, the results of the k splits are averaged to produce an accuracy score that more reliably indicates how the model will perform on unseen data.

Three train/test splits were used for the energized cable data and five for the unenergized cable data. The results of the splits were then averaged to represent the accuracy of the models. The data were split according to the case (e.g., connect end A, motor end B), so one case at a time is the test set and the rest constitute the training set. The same splits were used for the supervised and unsupervised models to allow for a fair comparison of the two.

4.3 Unsupervised Methods

The unsupervised method applied, called the “Pointwise” method, was adopted from previous work (Glass et al. 2023). The general idea behind the method is to calculate a distance metric such that for normal samples, the distance is expected to be small but will increase as the cable transitions to an anomalous state.

Conceptually, this method combines the set of possible anomalies into a single anomalous class, turning the problem into a binary classification problem of either normal or not normal (Chandola, Banerjee, and Kumar 2009). It then implements a one-class classification approach, meaning it learns strictly from the normal class to determine a boundary, or threshold, beyond which data are classified as anomalous. This approach has the benefit of not needing labeled data for each possible anomaly, which may be infeasible to obtain.

First, the data are split to produce a training set and a test set. Of the training samples, only the data pertaining to undamaged states are needed to produce a score (although anomalous training data are used later in selecting a decision threshold). To produce a score, a test sample is compared against the training set to compute a distance (discussed later in this section) from the training samples, which are assumed to be undamaged. Damaged cables will ideally have a significantly higher score (i.e., distance) than undamaged cables. The scores of the training split are used to find an optimal threshold that is used to predict the condition of the samples in the test split.

In the case of the pointwise model (Figure 17), the method calculates if the measurement at each point along the cable is like something that has been observed in the training set at that point. The test sample is compared against the training samples. At each point along the length of the cable the minimum difference to any training sample is selected, and the values from all evaluated points are averaged to produce a score. A different training sample could be selected at each point. If many measurements are different from what is in the training set, then the sample will receive a higher score than a sample for which values are similar to those of the training set at each point.

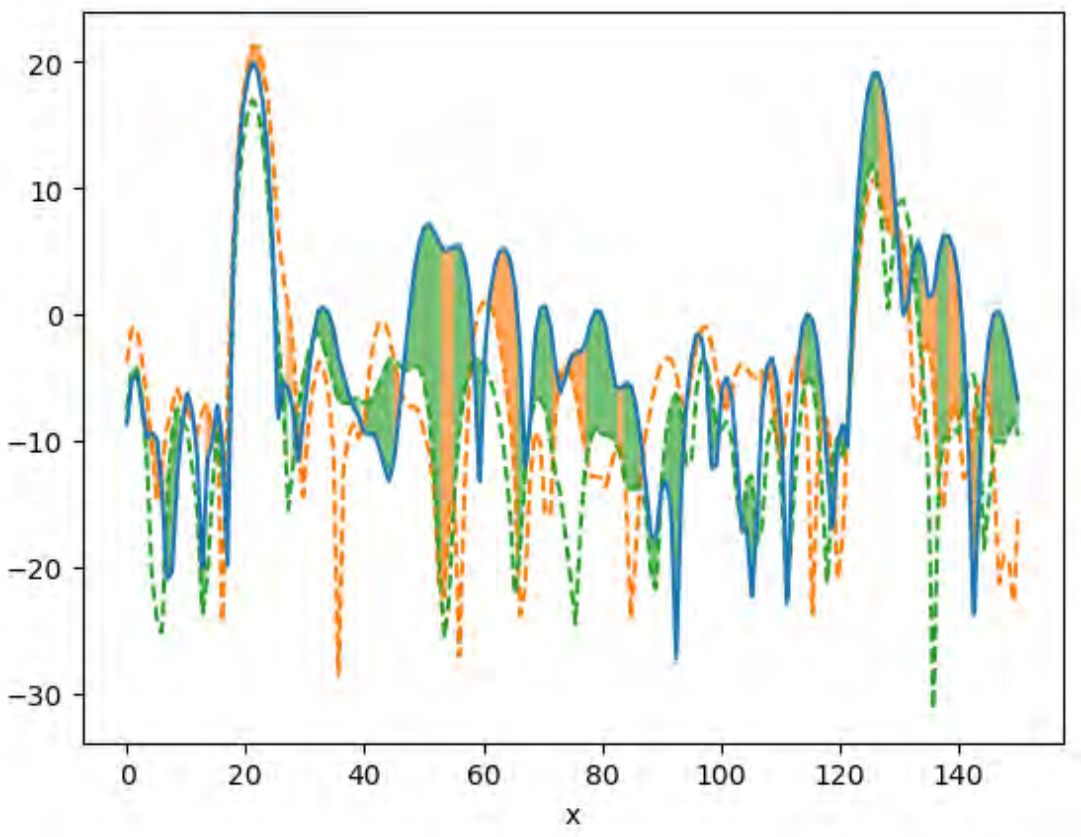

Figure 17. The Pointwise method is being applied to the solid blue line. The green and orange shading indicates which training sample is closer to the test sample at each point.

A decision threshold method was used to classify calculated scores as either normal or anomalous, with scores exceeding the threshold classified as anomalous. The optimal threshold to maximize performance was calculated using the normal and anomalous samples within the training set. For the normal samples, an iterative cross-validation approach was used because the approach used normal data for the model. At each iteration, one normal sample was withheld, and the remaining samples were used to score the held-out sample. For the anomalous samples, scores could be directly calculated using all the normal samples within the training set. Once all the scores were calculated, the threshold was selected as the value that maximizes the weighted accuracy (defined in Section 4.5). This threshold was then applied to the test set to evaluate the classification accuracy. Other methods could have been chosen to calculate this threshold. For example, if the training set included no anomalous samples, the cross-validation approach could be used to calculate scores for the normal training samples and the maximum score could be used as the threshold.

This distance-based model was selected for the present effort over more complicated unsupervised architectures like autoencoders (that make use of neural network architectures) because of the small size of the dataset. For data architectures based on neural networks to generalize well, they need significant amounts of data to learn to extract the patterns present in the data. Without sufficient data, these architectures are prone to memorize the limited training set and thus generalize poorly.

4.4 Supervised Methods

Supervised ML algorithms learn from labeled training data to make predictions or decisions without human intervention. In supervised learning, the algorithm is provided with a dataset consisting of input-

output pairs. The algorithm learns to map inputs to outputs. The FDR and SSTDR data from different bandwidths were analyzed similarly to the unsupervised methods. Extra Tree Classifier (ETC) supervised model was employed in this study to classify the anomaly, which also worked best in our previous study in terms of supervised models (Glass, et al. 2024b).

ETC is a popular machine learning algorithm used for both classification and regression tasks. It operates by recursively partitioning the dataset into subsets based on the values of input features, creating a tree-like structure of decisions. At each node of the tree, the algorithm selects the feature that best separates the data, typically using metrics like Gini impurity or information gain for classification tasks. The decision tree continues to split the data until it reaches a predefined stopping criterion, such as a maximum tree depth or a minimum number of data points per leaf. To make predictions, data points traverse the tree from the root node to a leaf node, where they are assigned the majority class label (for classification) or the mean value (for regression) of the training examples in that leaf (Wu et al. 2008). Decision Trees are interpretable and intuitive, capable of capturing complex interactions in the data, but they are prone to overfitting when not properly pruned or regularized.

4.5 Evaluation Metrics

This effort used the concept of weighted accuracy to report and compare the performance of different cable types, preprocessing methods, spectrometry methods, and frequencies. Accuracy was selected because it is highly interpretable compared to other classification metrics, making it a clear choice for a feasibility study. Weighted accuracy was specifically chosen because it averages the accuracy for each class individually, which is beneficial when there are unequal numbers of samples in the different classes. As an example, if there are 99 normal samples and one anomalous sample and all are labeled as normal, the accuracy would be $\frac{99}{100} = 0.99$, but the weighted accuracy would be $(\frac{99}{99} + \frac{0}{1})/2 = 0.5$.

Using the developed approaches, anomaly scores for each sample and combination of approach options were calculated. To convert these to weighted accuracies, thresholds had to be selected. For this feasibility study, thresholds were selected to maximize the weighted accuracies. While these are likely higher than would be seen in real conditions, they provide appropriate approximations of the weighted accuracies to determine whether the algorithms are working and to be able to compare the algorithms against each other.

5. RESULTS

5.1 Unsupervised Learning Results

The results of the unsupervised model were generated and analyzed to compare the effect of several instruments, frequencies, and preprocessing methods on the ability to differentiate damaged and undamaged medium voltage cables. The analysis demonstrates weighted accuracy consistent with the results of the model when applied to low-voltage cables. The unsupervised model was able to perform well on a few instruments, reaching a maximum of 93.8% weighted accuracy on the FDR Direct Connect data using 100 MHz and our real preprocessing method.

We first analyzed the instruments and corresponding methods of connecting them to the cable, as shown in Figure 18. This analysis showed that the Direct Connect and Iso-Coupled Unenergized methods produced significantly greater accuracy than the Iso-Coupled HV Diagnostics (HVD) Energized or Unenergized methods. This trend held true for both the SSTDR and the FDR.

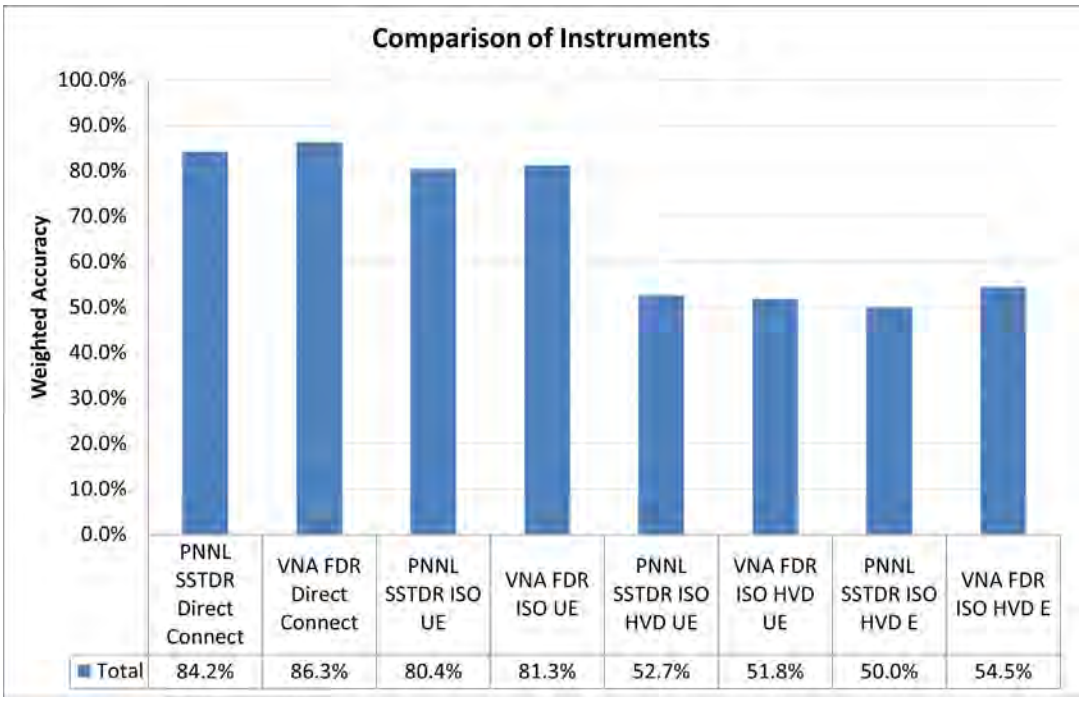

Figure 18. Comparison of instruments averaging across all frequencies and preprocessing methods.

Our next analysis investigated the impact of frequency on performance, as shown in Figures 19 and 20. The CWF preprocessing method combines all the frequencies measured, so it is presented as its own column. Figure 19 shows a correlation between frequency and accuracy, with higher frequencies performing better on medium voltage cables. Figure 20 shows an even stronger trend by focusing on the Direct Connect and Iso-Coupled Unenergized results, which were found to perform best. The CWF preprocessing method displays surprisingly high average accuracy, averaging 86.5% across the selected instruments.

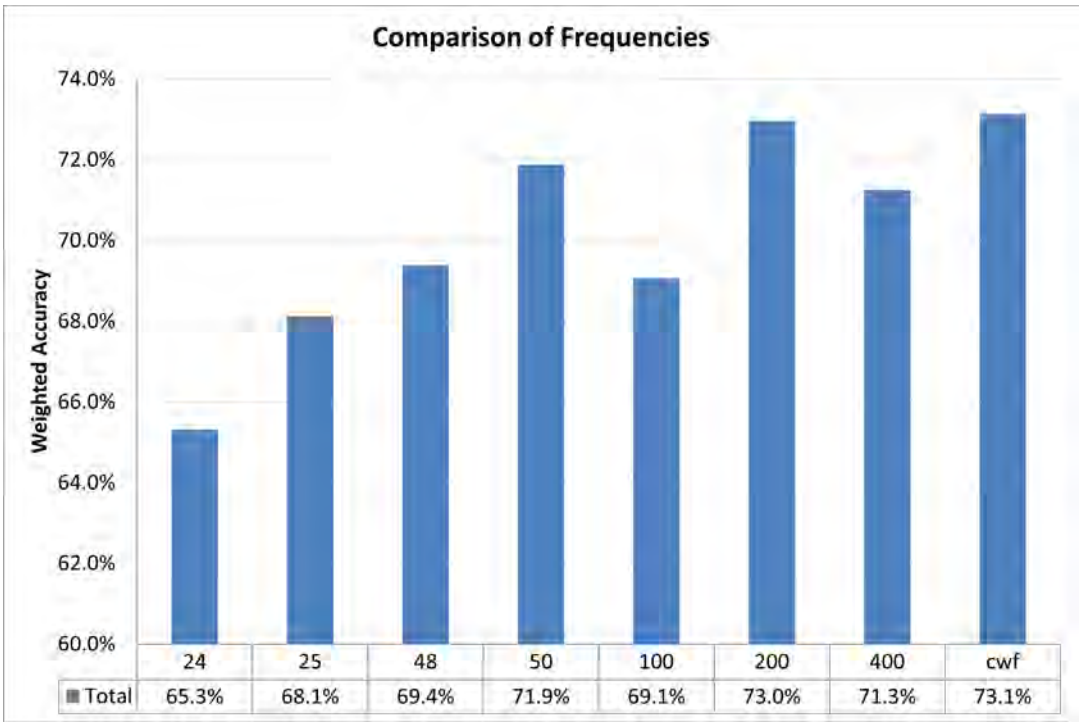

Figure 19. Comparison of frequencies averaging across all instruments and preprocessing methods.

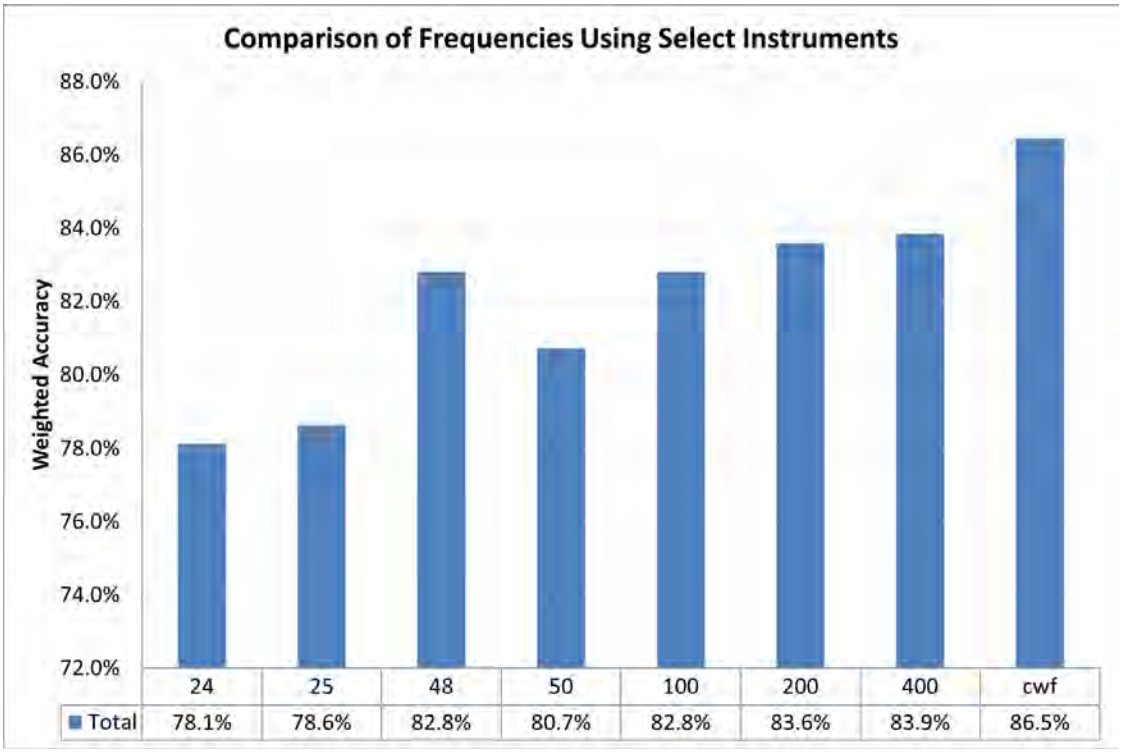

Figure 20. Comparison of frequencies averaging across all preprocessing methods and the best performing instruments.

Results can also be categorized by preprocessing method to assess how this is correlated with performance, as shown in Figure 21. Using the previously identified best instruments, our findings in

Figure 21 indicate that the real and imaginary preprocessing methods perform best while the complex magnitude preprocessing method performs worse. The CWF and magnitude preprocessing methods both present the data in A.U. rather than dB, which may explain why they perform similarly.

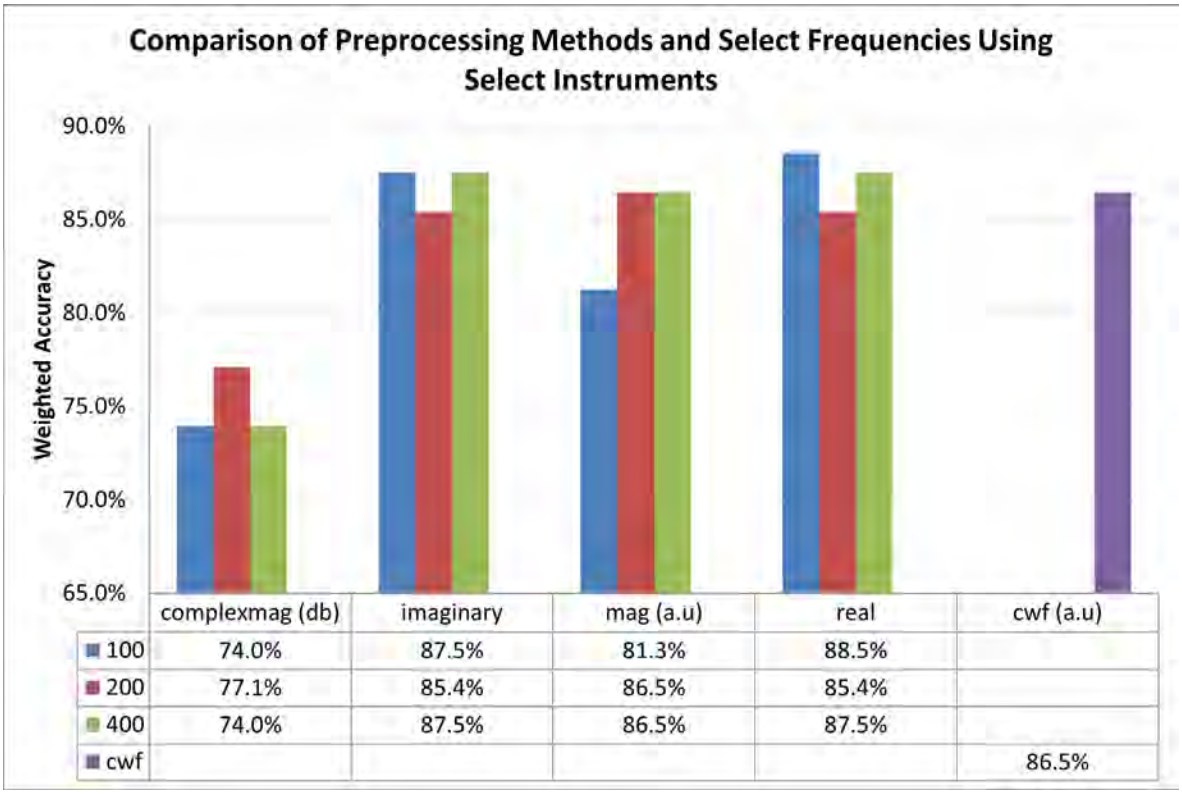

	complexmag (db)	imaginary	mag (a.u)	real	cwf (a.u)
100	74.0%	87.5%	81.3%	88.5%	
200	77.1%	85.4%	86.5%	85.4%	
400	74.0%	87.5%	86.5%	87.5%	
cwf					86.5%

Figure 21. Comparison of preprocessing methods using select frequencies and the best performing instruments.

In conclusion, the best results from the unsupervised model use the Direct Connect or Iso-Coupled Unenergized connection methods in conjunction with high frequency.

5.2 Supervised Learning Results

The results of the supervised model were analyzed to compare the effect of several instruments, frequencies, and preprocessing methods on the ability of the model to differentiate damaged and undamaged medium voltage cables. Like the unsupervised model, the supervised model performed well on the FDR Direct Connect instrument configuration with a weighted accuracy of 80.6% when we consider all the frequencies to train the model across all the instruments as presented in Figure 22. The second-best performing instrument configuration was the VNA FDR Iso-Coupled Unenergized with a weighted accuracy of 77%. In contrast, the SSTDR instrument configurations performed poorly in terms of weighted accuracy for the supervised models.

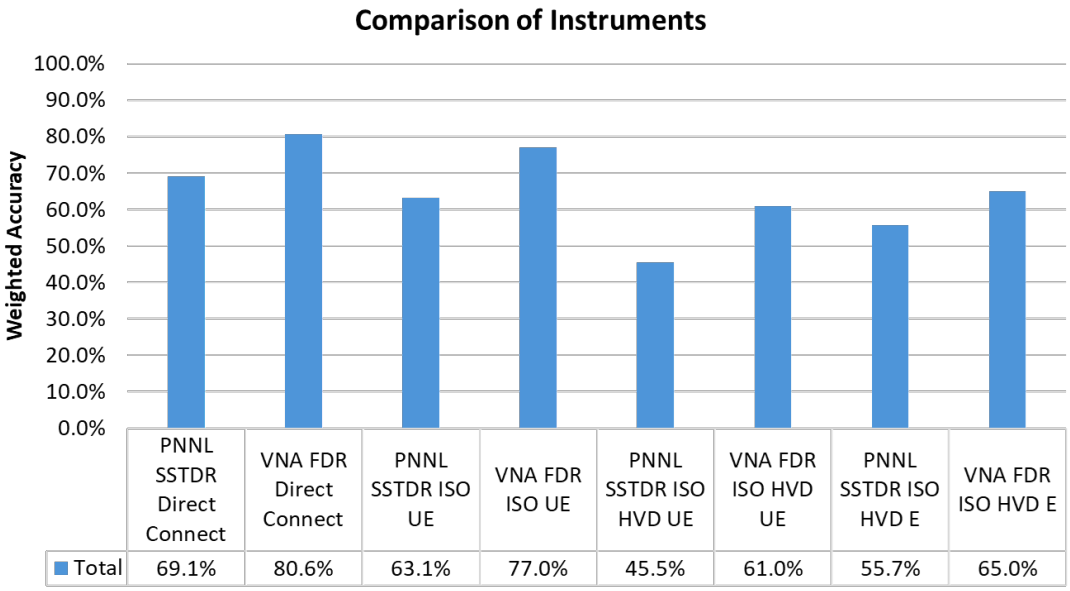

Figure 22. Comparison of instruments averaging across all frequencies and preprocessing methods.

Our analysis also shows that frequency has a significant impact on the result. Figure 23 shows a correlation between frequency and accuracy, with higher frequencies performing better on medium voltage cables. However, for the best performing instrument configuration (VNA FDR Direct Connect) the supervised model shows the minimum effect of frequencies on the weighed accuracy as presented in Figure 24. For this case frequencies 50, 100, 200 and 400 MHz perform almost in the same range of weighted accuracy.

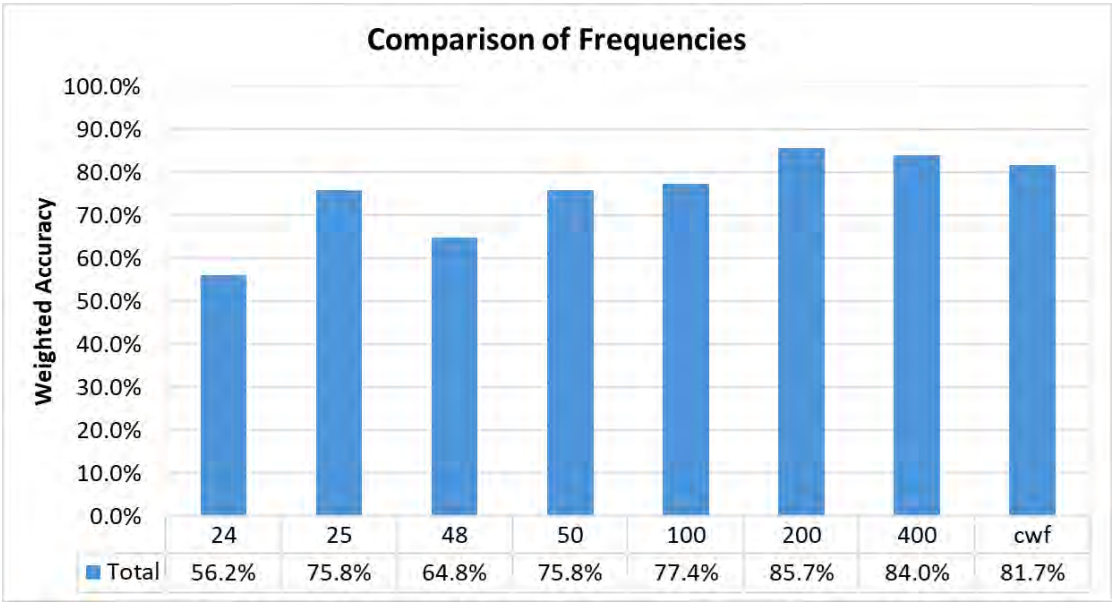

Figure 23. Comparison of frequencies averaging across all instruments and preprocessing methods.

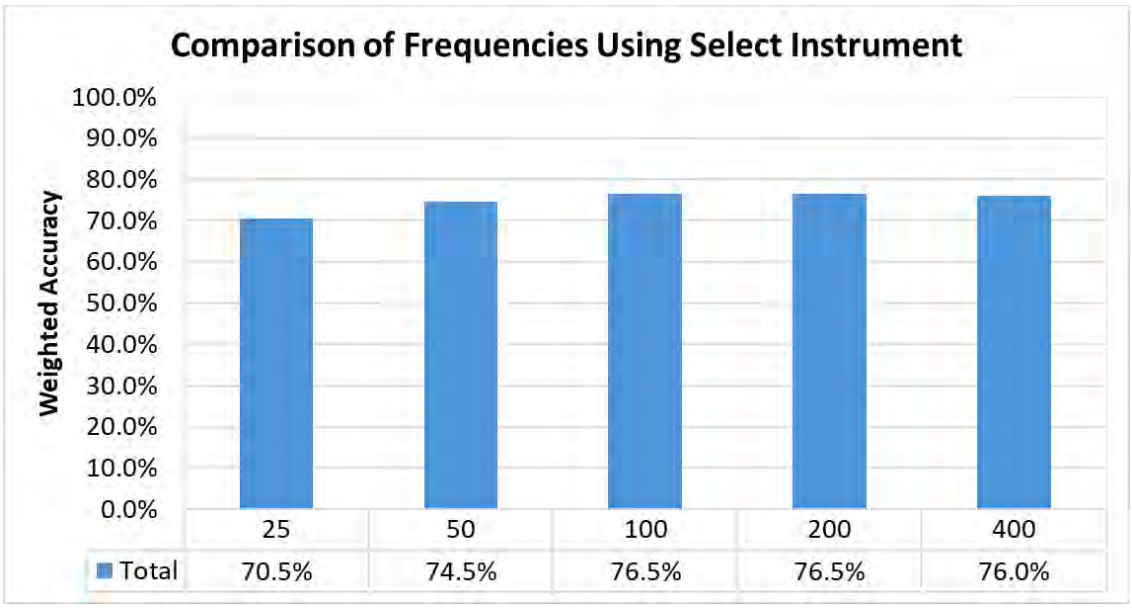

Figure 24. Comparison of frequencies averaging across all preprocessing methods and the best performing instrument.

Results can be categorized by preprocessing method to assess how performance is correlated with better-performing frequencies, as presented in Figure 25. Frequencies of 100, 200, and 400 MHz for the VNA FDR Direct Connect instrument configuration are considered in this analysis. For the unsupervised method, each frequency was trained separately, as shown in Figure 21. However, when each frequency was treated separately for the supervised method, the data size was significantly reduced, which is considered a limitation of the supervised method. To address this limitation, the 100, 200, and 400 MHz frequencies for the VNA FDR Direct Connect instrument configuration were merged to evaluate the performance of each preprocessing method, as presented in Figure 25. Using the previously identified best performing instrument configuration (VNA FDR Direct Connect) and better performing frequencies, the findings in Figure 25 indicate that all preprocessing methods achieve nearly similar weighted accuracy, ranging between 78% and 81%.

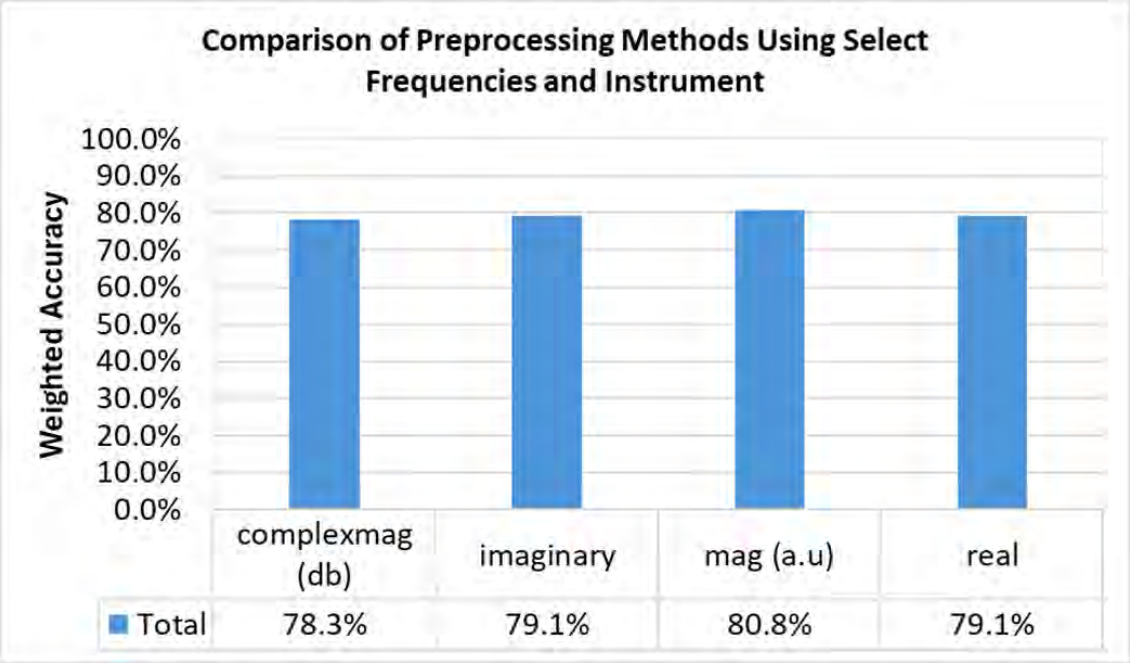

Figure 25. Comparison of preprocessing methods using select frequencies and the best performing instrument.

6. OBSERVATIONS

6.1 Extending Models to Other Lengths of Cable

One limitation of these models is that they require data to be collected for each length of cable. For example, a 200 ft cable cannot be analyzed using data collected from 100 ft cables. Rather, it would need data from 200 ft cables to compare against. To address this shortcoming, several methods were tested. Broadly, the methods tested include linear interpolation, sequence alignment, and computer vision.

The unsupervised method was tested on different lengths of cable using linear interpretation to scale data from different cables. Data corresponding to cables of different lengths were scaled and interpolated such that the shorter cable had the same number of data points as the longer cable. This yielded results of around 50% weighted accuracy for the unsupervised method and from 22 to 61% using the supervised method.

The linear interpolation approach was taken a step farther using a DTW. After the shorter cable was stretched to have more points, DTW was applied to align the data of the shorter cable with the data of the longer cable. Visually, the alignment of cables using DTW was successful. However, the unsupervised method could not distinguish between undamaged and damaged cables. We suspect that the actual noise from damaged portions of the cables was aligned with the random noise that can be seen in all cables. This made damaged cables indistinguishable from undamaged cables.

A different approach that was tested involved a Convolutional Neural Network (CNN) that had been pretrained for classification on ImageNet, a large database of images. The CNN was configured to take figures of cable reflectometry data as input and output to generate a prediction of damaged or undamaged. However, the model performed poorly with a weighted accuracy of 41%. This method was not tested exhaustively and may be able to provide better results by altering the model architecture differently, using

different crops of the cable data images, or even using more subtle approaches like changing the color of the line in the images.

6.2 Using Low Voltage-Medium Voltage: Supervised Model

Like unsupervised models, the main limitation of supervised methods is that the same number of features are required for training a model. Problems are encountered when cables of different lengths are used. For instance, when a 200 ft cable is preprocessed at 0.25 ft intervals, it results in 800 data points, whereas preprocessing an 80 ft cable would yield only 320 data points. Therefore, to train a model on a 200 ft low voltage cable and test the model on an 80 ft medium voltage cable, the data must be preprocessed in a manner that ensures a similar number of data points for both training and testing sets. Linear interpolation was applied to downsize the data points for the 200 ft cable to test it on the 80 ft cable. However, the methods performed poorly, with weighted accuracy ranging from 22% to 61%, depending on the preprocessing techniques used.

7. CONCLUSIONS

This study aimed to address the need for efficient and effective condition monitoring of installed aging cables. The wholesale replacement of NPP cables is cost-prohibitive, and experience has shown that cables can function safely beyond their initial qualification. Reflectometry techniques, combined with ML methods, offer promising tools for assessing cable conditions in a non-intrusive and efficient manner. This study builds on previous research to apply supervised and unsupervised ML models to differentiate between damaged and undamaged medium voltage cables, with the goal of improving diagnostic accuracy and efficiency.

The unsupervised model achieved a maximum weighted accuracy of 93.8% using VNA FDR Direct Connect data at 100 MHz with real preprocessing. The analysis indicated that Direct Connect and Iso-Coupled Unenergized methods produced significantly higher accuracy compared to other connection methods. Furthermore, higher frequencies correlated with better performance, especially when using the Direct Connect and Iso-Coupled Unenergized methods. Among preprocessing methods, real and imaginary preprocessing performed best, while the complex magnitude preprocessing method performed the worst.

For the supervised model, the maximum weighted accuracy achieved was 80.6% using the VNA FDR Direct Connect configuration with all frequencies. Like the unsupervised model, the Direct Connect and Iso-Coupled Unenergized methods produced higher accuracy compared to other methods, and higher frequencies generally correlated with better performance, though for the VNA FDR Direct Connect configuration, frequencies of 50, 100, 200, and 400 MHz performed similarly. However, in contrast to the unsupervised model, preprocessing methods did not have much impact on performance.

When comparing the unsupervised and supervised models, it is evident that the unsupervised model generally achieved higher accuracy, peaking at 93.8%, compared to 80.6% for the supervised model. This discrepancy may be attributed to the nature of many anomalies, where supervised methods tend to learn to differentiate between instances in the training set but may not generalize as well to unseen anomalies.

One of the significant challenges in this type of work is the difficulty in collecting data, as different cable lengths, voltages, materials, construction methods, and real-world conditions are likely to present varying conditions. This variability makes it challenging to extract generalizable characteristics, which is essential for taking full advantage of collected data. Supervised methods, in particular, face implementation difficulties because they rely heavily on the ability to extract information from collected data to generalize to unseen conditions.

To address this, our proposed pipeline for practical application leverages unsupervised methods. By training on the initial reading of each cable, we establish a baseline measurement. Any deviations or degradation from this baseline can be detected and flagged, providing a method to monitor the cable condition over time. Based on our studies of both low and medium voltage cables, these unsupervised methods have proven to be extremely accurate and robust, capable of handling many different types of anomalies. Furthermore, they can even quantify the degradation, as demonstrated in the thermal aging studies of previous research (Glass et al. 2024c). However, it is important to note that this approach may not detect pre-existing damage that was present before the initial baseline reading was taken, highlighting the inherent challenges of the problem.

Overall, this study demonstrates that the unsupervised methods previously developed for low voltage cables extend effectively to medium voltage cables, showcasing the robustness of the framework and approaches. These findings can serve as a guideline for commercial applications, aiding in the development of technologies that enable efficient and effective cable condition monitoring and condition-based qualification of cables, ultimately enhancing the reliability and safety of nuclear power plant operations.

Page intentionally left blank

8. REFERENCES

Chandola, V., A. Banerjee, and V. Kumar. 2009. "Anomaly Detection: A Survey." *ACM Computing Surveys* 41 (3): 1-58. Article 15. https://doi.org/10.1145/1541880.1541882.

Copper Mountain. 2020. "TR1300/1 2-Port 1.3 GHz Analyzer." Accessed August 29, 2022. https://coppermountaintech.com/vna/tr1300-1-2-port-1-3-ghz-analyzer/.

Edun, A. S., C. LaFlamme, S. R. Kingston, C. M. Furse, M. A. Scarpulla, and J. B. Harley. 2022. "Anomaly Detection of Disconnects Using SSTDR and Variational Autoencoders." *IEEE Sensors Journal* 22 (4): 3484-3492. https://doi.org/10.1109/JSEN.2022.3140922.

Edun, A. S., C. LaFlamme, S. R. Kingston, H. V. Tetali, E. J. Benoit, M. Scarpulla, C. M. Furse, and J. B. Harley. 2021. "Finding Faults in PV Systems: Supervised and Unsupervised Dictionary Learning With SSTDR." *IEEE Sensors Journal* 21 (4): 4855-4865. https://doi.org/10.1109/JSEN.2020.3029707.

Furse C., Y. C. Chung, R. Dangol, M. Nelsen, G. Mabey, and R. Woodward. 2003. "Frequency Domain Reflectometry for On-Board Testing of Aging Aircraft Wiring." *IEEE Transactions on Electromagnetic Compatibility* 45 (2): 306-315. https://doi.org/10.1109/TEMC.2003.811305.

Furse C., Y. C. Chung, C. Lo, P. Pendayla. 2006. "A Critical Comparison of Reflectometry Methods for Location of Wiring Faults." *Smart Structures and Systems* 2 (1): 25-46. https://doi.org/10.12989/sss.2006.2.1.025.

Glass S.W., L.S. Fifield, G. Dib, J.R. Tedeschi, A.M. Jones, and T.S. Hartman. 2015. *State of the Art Assessment of NDE Techniques for Aging Cable Management in Nuclear Power Plants FY2015.* Pacific Northwest National Laboratory PNNL-24649. Richland, WA. https://doi.org/10.2172/1242348.

Glass, S. W., A. M. Jones, L. S. Fifield, and T. S. Hartman. 2017. "Frequency Domain Reflectometry NDE for Aging Cables in Nuclear Power Plants." *AIP Conference Proceedings* 1806: 080015. https://doi.org/10.1063/1.4974640.

Glass, S. W., M. P. Spencer, L. S. Fifield, A. Sriraman, and M. S. Prowant. 2021a. *Nondestructive Evaluation (NDE) of Cable Moisture Exposure Using Frequency Domain Reflectometry (FDR).* Pacific Northwest National Laboratory PNNL-31934. Richland, WA. https://doi.org/10.2172/1820614.

Glass, S.W., L S. Fifield, and M Prowant. 2021b. *PNNL ARENA Cable Motor Test Bed Update.* Pacific Northwest National Laboratory PNNL 31415. Richland, WA. https://doi.org/10.2172/1870432.

Glass, S.W., A. Sriraman, M. Prowant, M. P. Spencer, L.S. Fifield, and S. Kingston. 2022. *Nondestructive Evaluation (NDE) of Cable Anomalies using Frequency Domain Reflectometry (FDR) and Spread Spectrum Time Domain Reflectometry (SSTDR).* Pacific Northwest National Laboratory PNNL-33334. https://doi.org/10.2172/2203543.

Glass, S.W., J. Tedeschi, M.P. Spencer, J. Son, D. Li, M. Elen, and L. S. Fifield. 2023 .*Extended Bandwidth Spread Spectrum Time Domain Reflectometry Cable Test for Thermal Aging, Low Resistance Fault, and Water Detection.* Pacific Northwest National Laboratory PNNL-34815. https://doi.org/10.2172/2203239.

Glass, S. W., J. R. Tedeschi, M. Elen, M. P. Spencer, J. Son, V. Kumar, and L. S. Fifield. 2024a. *Evaluation of Clamshell Current Coupler for Online Frequency Domain and Spread Spectrum Time Domain Reflectometry to Detect Anomalies in Energized Cables.* Pacific Northwest National Laboratory PNNL-36530. Richland WA. https://www.pnnl.gov/publications/evaluation-clamshell-current-coupler-online-frequency-domain-and-spread-spectrum-time.

Glass, S.W., J.R. Tedeschi, M. Elen, J. Son, M. Taufique, V. Kumar, K. Hasan, S. Kumari, T. Tueller, M.P. Spencer, L.S. Fifield, A. Kaforey, J. A. Farber, A. Al Rashdan. 2024b. *SSTDR and FDR Detection of Un-Energized and Energized Cable Anomalies Including Thermal Degradation Using Machine Learning.* Pacific Northwest National Laboratory PNNL-36573. Richland, WA. https://www.pnnl.gov/main/publications/external/technical_reports/PNNL-36573.pdf.

Glass, S.W., J.R. Tedeschi, M.P. Spencer, J. Son, M. F. N. Taufique, D. Li, M. Elen, L. S. Fifield, J. A. Farber, and A. Al Rashdan. 2024c. "Spread Spectrum Time Domain Reflectometry (SSTDR) and Frequency Domain Reflectometry (FDR) Cable Inspection Using Machine Learning." In *Proceedings of the 2024 51st Annual Review of Progress in Quantitative Nondestructive Evaluation*. ASME, Denver, Colorado, July 21–24, 2024. https://doi.org/10.1115/QNDE2024-133645.

Glass, S. W., J. R. Tedeschi, M. Elen, M. P. Spencer, J. Son, and L. S. Fifield. 2025. "Clamshell Inductive Current Coupler for Online Cable Condition Monitoring." *IEEE Open Journal of Instrumentation and Measurement* 4:1-8. 6000108. https://doi.org/10.1109/OJIM.2024.3517623.

IAEA. 2017. *Benchmark Analysis for Condition Monitoring Test Techniques of Aged Low Voltage Cables in Nuclear Power Plants: Final Results of a Coordinated Research Project.* International Atomic Energy Agency IAEA-TECDOC-1825. Vienna, Austria. https://www.iaea.org/publications/11164/benchmark-analysis-for-condition-monitoring-test-techniques-of-aged-low-voltage-cables-in-nuclear-power-plants.

IEEE. 2015. *IEEE Standard for Qualifying Electric Cables and Splices for Nuclear Facilities.* IEEE Standards Association IEEE 383-2015. Piscataway, NJ. https://doi.org/10.1109/IEEESTD.2015.7287711.

Kingston, S., E. Benoit, A. S. Edun, F. Elyasichamazkoti, D. E. Sweeney D, J. B. Harley, P. K. Kuhn, and C. M. Furse. 2021. "A SSTDR Methodology, Implementations, and Challenges." *Sensors* 21 (16): 5268. https://doi.org/10.3390/s21165268.

Lee, C.-K, and S. J. Chang. 2020. "Fault Detection in Multi-Core C&I Cable via Machine Learning Based Time-Frequency Domain Reflectometry." *Applied Sciences* 10 (1):158. https://doi.org/10.3390/app10010158.

Lim, H., G.-Y. Kwon, and Y.-J. Shin. 2021. "Fault Detection and Localization of Shielded Cable via Optimal Detection of Time–Frequency-Domain Reflectometry." *IEEE Transactions on Instrumentation and Measurement* 70:1-10. https://doi.org/10.1109/TIM.2021.3092514.

NRC. 1977. *Qualification Tests of Electric Cables, Field Splices, and Connections for Light-Water-Cooled Nuclear Power Plants.* Nuclear Regulatory Commission R-G 1.131. Washington, D. C. https://www.nrc.gov/docs/ml0037/ML003740128.pdf.

Okonite. 2019. "The Master Catalog of Okonite Cables." https://www.okonite.com/product-catalog/section-2.

Robles, G., M. Shafiq, and J. M. Martinez-Tarifa. 2019. "Multiple Partial Discharge Source Localization in Power Cables Through Power Spectral Separation and Time-Domain Reflectometry." *IEEE Transactions on Instrumentation and Measurement* 68 (12): 4703-4711. doi: https://doi.org/10.1109/TIM.2019.2896553.

Slimani, H., Y. Gargouri, F. M. N. Mboula, and N. Ravot. 2024. "Machine Learning Approach for Classification of Faults in Cable via Compressed Sensing Time-Domain Reflectometry." In *2024 Prognostics and System Health Management Conference (PHM)* Stockholm, Sweden, May 28-31, 2024. https://doi.org/10.1109/PHM61473.2024.00061.

Wu, X., V. Kumar, J. R. Quinlan, J. Ghosh, Q. Yang, H. Motoda, G. J. McLachlan, A. Ng, B. Liu, P. S. Yu, Z.-H. Zhou, M. Steinbach, D. J. Hand, and D. Steinberg. 2008. "Top 10 Algorithms in Data Mining." *Knowledge and Information Systems* 14 (1): 1-37. https://doi.org/10.1007/s10115-007-0114-2.

Yao, L., W. Ma, and C. Yu. 2014. "Correlation Between Transfer Impedance and Insertion Loss of Current Probes." *IEEE Electromagnetic Compatibility Magazine* 3: 51-55. https://doi.org/10.1109/MEMC.2014.6849544.